

Horizontal deflection of single particle in a paramagnetic fluid

S. Liu^{1,a}, Xiang Yi², M. Leaper³, and N.J. Miles⁴

¹ Process and Environmental Research Division, Faculty of Engineering, University of Nottingham, University Park, Nottingham, NG7 2RD, UK

² Research Institute of Sun Yat-Sen University in Shenzhen, Hi-tech Industrial Park, Shenzhen, 518057, China

³ Chemical Engineering and Applied Chemistry, Aston University, Birmingham B4 7ET, UK

⁴ Faculty of Science and Engineering, University of Nottingham Ningbo China, Taikang East Road, Ningbo, 315100, China

Received 10 October 2013 and Received in final form 18 April 2014

Published online: 6 June 2014 – © EDP Sciences / Società Italiana di Fisica / Springer-Verlag 2014

Abstract. This paper describes the horizontal deflection behaviour of a single particle in paramagnetic fluids under a high-gradient superconducting magnetic field. A glass box was designed to carry out experiments and test assumptions. It was found that the particles were deflected away from the magnet bore centre and particles with different density and/or susceptibility settled at a certain position on the container floor due to the combined forces of gravity and magneto-Archimedes as well as lateral buoyant (displacement) force. Matlab was chosen to simulate the movement of the particle in the magnetic fluid, the simulation results were in good accordance with experimental data. The results presented here, though, are still very much in their infancy, which could potentially form the basis of a new approach to separating materials based on a combination of density and susceptibility.

1 Introduction

Magnetic phenomena have been known and exploited for many centuries [1]. Many kinds of magnetic separation techniques, such as beneficiation of iron ore, recovery of metal from waste material, attraction of very small ferromagnetic particles onto steel filter wires (high gradient magnetic separation, HGMS), biomagnetic extraction of heavy metals and so on, have been developed and applied in industry. However, these techniques are restricted to treating ferromagnetic substances as the separation criteria are based on their pulsion/attraction towards the magnetic field [2–8].

Recently, the levitation of materials has become a topic of interest to a broad section of researchers [9]. There are two ways to levitate feeble magnetic substances, diamagnetic levitation and magneto-Archimedes levitation. The diamagnetic levitation of bismuth [10], the lifting of water [11] as well as the stable levitation of living frogs [12, 13] have been reported. The magneto-Archimedes effect was first noted by Braunbeck in 1939 [10]. Since then much work has been carried out and continued; Ikezoe *et al.* successfully levitated KCl and NaCl grains in pressurized oxygen gas [14] and also a 1 cm diameter water drop in the centre of a 10 Tesla magnet and levitated and separated Ti, C and S in 2.67 mol/l solution of dysprosium nitrate [15]. This highlights the importance of the

paramagnetic fluid (magneto-Archimedes agent) in providing the additional force to enable the particles to levitate. In addition, Hirota *et al.* [16] in 2004 successfully used magneto-Archimedes separation to separate biological materials.

Comparing the two methods, the levitation of diamagnetic objects requires very large magnetic field-gradient products due to the small magnetic susceptibility of the diamagnetic materials, thus there are only a limited number of materials which could be diamagnetically levitated and only limited laboratories in the world could do this work [14].

In the presence of a background fluid, magneto-Archimedes levitation applies the buoyancy principle to the levitation in a magnetic field, which could be modified as shown by the following equation [14]:

$$\frac{\chi_0}{\mu_0} B \frac{dB}{dz} - \rho_0 g - \frac{\chi_f}{\mu_0} B \frac{dB}{dz} + \rho_f g = 0, \quad (1)$$

where χ_0 and ρ_0 are the magnetic susceptibility and density of the levitating object respectively, χ_f and ρ_f are those of the background fluid. In diamagnetic levitation, the latter two terms on the left-hand side in eq. (1) have been neglected. For the vertical direction magnet field gradient, the particle will endure four types of forces. Similar to wood in water, the particle in the media around it will receive a weight and buoyancy force provided by the media. Also the particle will be influenced by two

^a e-mail: liushixiao8@hotmail.com

further types of force, magnetic attraction and the magnetic levitation, which are related to the magnetic field strength. Here the levitation is known as the magneto-Archimedes effect and the media called the magneto-Archimedes agent [17–19].

Mir *et al.* [20] pioneered the use of ferrohydrostatic separators in 1973 by employing a kerosene-based ferrofluid to separate automobile scrap [20]. Considerable effort to develop this technology was subsequently expended in Japan and USA with a comprehensive review of the history of FHS in Japan and USA given by Fujita [21]. FHS technology has been used in industry to process gold and PGM concentrates as well as for diamond beneficiation but at a limited scale [22]. However, the fluids lack stability in contact with the atmosphere and the magnetic fluids are black in colour making the recovery and regeneration of the fluid a challenge, all of which must be addressed for large scale industrial implementation.

With the development of the design and synthesis of superconductivity material, it will be possible to generate high magnetic fields at low cost and weakly magnetic fluids could replace the current ferrofluids [1]. Over the past decade a considerable amount of research has been conducted at the University of Nottingham on the levitation of particles under high magnetic fields and gradients [23–25]. An interesting phenomenon was noticed during some of the levitation experiments, that the particles were repulsed to the wall of a container to form a ring around the centre of magnetic. This paper is based on this phenomenon and explores a horizontal direction magnetic deflection system, which potentially provides a new concept to separate particles with different density and magnetic susceptibility. A model has been set up to simulate the phenomenon of deflection, which shows good accordance with the experimental results.

2 Experimental procedure

2.1 Materials

Manganese (II) chloride aqueous solution was used as the magnetic fluid during the experiments.

Different concentrations of MnCl_2 solution could be prepared (*i.e.*, 2 M, 3 M and 4 M) by dissolving the MnCl_2 crystal in distilled water to get a clear pink solution. The mass susceptibility of the MnCl_2 solution at 2 M, 3 M, 4 M can be obtained by calculation from Andres [26], which stated that the mass susceptibility of an aqueous solution of a paramagnetic salt could be obtained from the formula below [26]:

$$x_{\text{total}} = C_{\text{salt}}x_{\text{salt}} + (1 - C_{\text{salt}}) \times x_{\text{water}}, \quad (2)$$

$$C_{\text{salt}} = \frac{m_{\text{salt}}}{m_{\text{total}}}. \quad (3)$$

The susceptibilities of MnCl_2 x_{salt} and water x_{water} are given as 114×10^{-6} and $-0.724 \times 10^{-6} \text{ cm}^3 \text{ g}^{-1}$ in cgs units, respectively [26–29]. The volume susceptibility (k) of a 2M MnCl_2 solution can be obtained by satisfying the

Table 1. The density and volume magnetic susceptibility of different concentrations manganese (II) chloride solution.

Solution	Density (kg m^{-3})	$k \times 10^{-6}$
2 M Manganese (II) chloride	1227	345
3 M Manganese (II) chloride	1301	502
4 M Manganese (II) chloride	1395	660

following below formulas:

$$x_{\text{salt}} = \frac{m_{\text{salt}}x_{\text{salt}} + m_{\text{water}}x_{\text{water}}}{m_{\text{salt}} + m_{\text{water}}}, \quad (4)$$

$$k = \rho x \times 4\pi \times 10^{-3}. \quad (5)$$

The corresponding volume magnetic susceptibility of 2 M, 3 M and 4 M MnCl_2 solution could be calculated and summarised in table 1.

From table 1, a 4 mol/l MnCl_2 solution has the density and susceptibility of 1395 kg m^{-3} and $6.6 \times 10^{-4} \text{ m}^3 \text{ kg}^{-1}$, respectively, which was used in all the following experiments where it was required. A range of well-defined particulate materials was used including pyrite and glass spheres. The physical properties of the pyrite and glass spheres used in the experiments are listed in table 2. The diameter of glass particles in this paper is exactly 1 mm and 0.7 mm for each value of B , not the average or range. The pyrite particles diameter ranges from 0.7 to 1.2 mm.

2.2 Superconducting magnet

The experiments were performed using an Oxford Instruments Minimum Condensed Volume (MCV) superconducting magnet, which had a 5 cm diameter open bore with the maximum magnet central field being about 17 T in the magnet bore, and the maximum $B \frac{dB}{dz}$ (BB') field gradient about $\pm 1470 \text{ T}^2 \text{ m}^{-1}$. The picture of the superconducting magnet is shown in fig. 1a. The maximum field strength position is about 19 cm down into the bore from the top plate of the superconducting magnet. The magnet field strength from the top plate of the superconducting magnet rig is shown in fig. 1b.

2.3 Design of glass box

As observed in the trial tests, the particles levitated in the magneto-Archimedes fluid were repulsed to the wall of a container in the superconducting magnet field centre area.

In order to explore this interesting behaviour, a rectangular glass box was made with dimensions, $145 \times 195 \times 25$ mm. The box was placed on top of the magnet as shown in fig. 2 with one of the end faces being positioned over the centre of the magnet bore. This was the point where the particles were fed or introduced into the fluid.

2.4 Data collection

When a single particle was placed into the liquid at the end of the box close to the magnet bore centre as shown in

Table 2. Physical properties of pyrite and glass spheres.

Materials	Particle size	Density (kg m ⁻³)	$k_p \times 10^{-6}$	$x_p \times 10^{-9} \text{ m}^3 \text{ kg}^{-1}$
Pyrite	0.7–1.2 mm	5000	338	67.5
Glass spheres	0.7 and 1.0 mm	2472	(-)	(-)

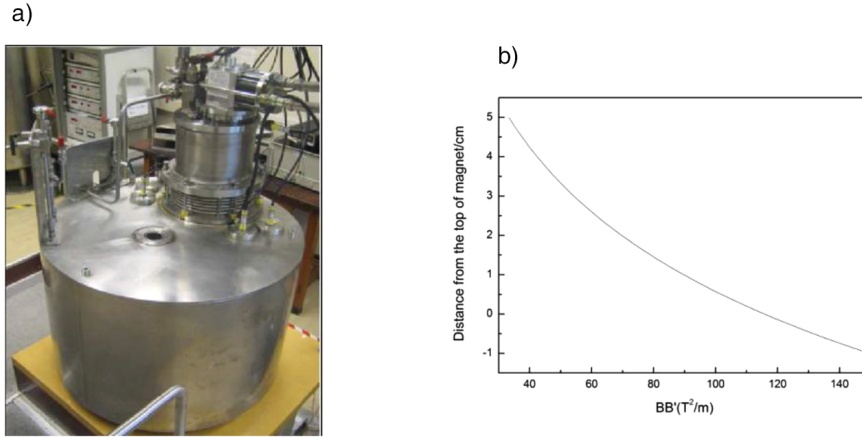


Fig. 1. MCV magnet system used in experiments. a) MCV magnet system. b) BB' vs. distance from the top of magnet.

fig. 2, a video camera Trust WB-3500T was used to record the movement of the particle. The hardware resolution of it is 640×480 pixels (300 K) and the camera can take up to 30 frames per second. And then the video was decomposed to frames by software Ulead Videostudio. The individual frame with 0.1 second time lapse interval was analysed to extract the path of particle during deflection.

2.5 Numerical simulation details

2.5.1 Equilibrium of a particle in a magneto-Archimedes solution

MATLAB is a numerical computing environment and fourth-generation programming language, recently many researchers used this kind of software to develop the numerical modelling in engineering areas [30–33]. Numerical simulation of particle behaviour in a magnetic field was carried out to explore the deflection phenomena during the single particle experiments using Matlab software. To find a suitable model to simulate the process, the first step was to calculate the equilibrium of a particle in a magneto-Archimedes solution. To analyze the detailed forces acting on the particle, the forces were extracted to horizontal direction force F_r and vertical direction force F_z . From the equation of magnetic energy [13]

$$\frac{B^2}{2\mu_0} \frac{dU_{\text{mag}}}{dB} = kV \frac{B}{\mu_0} \tag{6}$$

By the chain rule, the form of F_r and F_z can be acquired as below [34]:

$$F_z = \frac{dU}{dz} = \frac{dU_{\text{mag}}}{dB} \cdot \frac{dB}{dz} = \frac{kVB}{\mu_0} \cdot \frac{dB}{dz} \tag{7}$$

$$F_r = \frac{kVB}{\mu_0} \cdot \frac{dB}{dr} \tag{8}$$

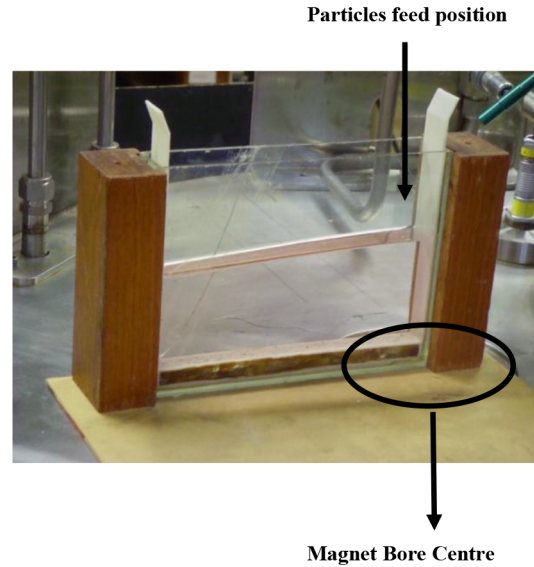


Fig. 2. Experimental setup with glass container.

The above vertical force is just the magnetic vertical direction force. But actually the particle in the magneto-Archimedes fluid should stand the buoyancy force provided by the solution. Combining the gravity and buoyancy, the vertical direction force in total could be summarised as below [24]

$$F_z = (k_p - k_l)VB \frac{dB}{dz} \cdot \frac{1}{\mu_0} - (\rho_P - \rho_l)Vg. \tag{9}$$

The horizontal direction force also could be summarised as the following formula considering the solution effect:

$$F_r = (k_p - k_l)VB \frac{dB}{dr} \cdot \frac{1}{\mu_0} \tag{10}$$

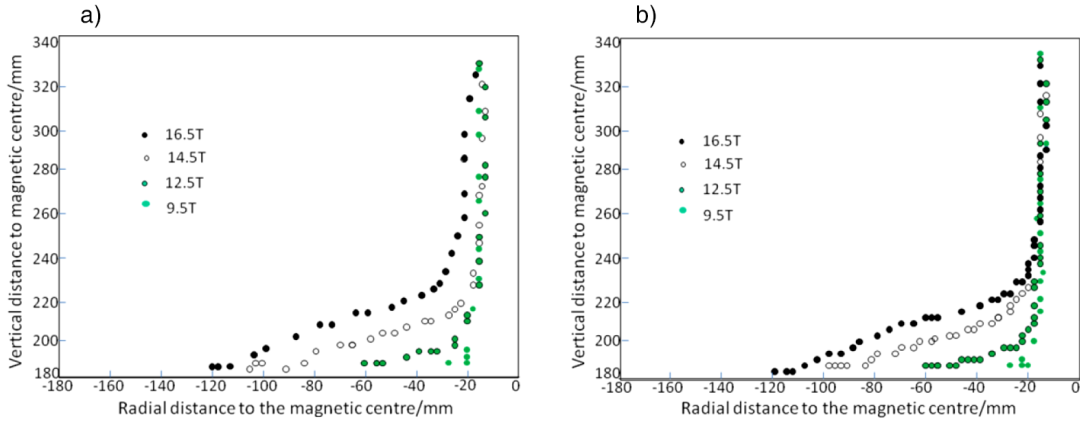


Fig. 3. The deflection of glass particle under different magnetic field. a) Glass particle with $d = 1$ mm. b) Glass particle with $d = 0.7$ mm.

The total magnetic field strength of every position is the combination of horizontal and vertical direction magnetic field strength as shown below, where Z means the vertical direction and r means the horizontal direction

$$B = \sqrt{B_z^2 + B_r^2}. \quad (11)$$

In the above equation, the total magnetic field strength B and vertical direction magnetic field gradient $\frac{dB}{dz}$, horizontal direction magnetic field gradient $\frac{dB}{dr}$ can be measured on site. Based on the measured magnetic field strength data, the force of the particles could be calculated.

2.5.2 Horizontal deflection simulation

For a better understanding of the deflection paths of the particle in 4M MnCl_2 , in this section we will simulate the displacement of the particle numerically by considering that the motion of each particle is mainly caused by F_z and F_r . In our case, these two mutually orthogonal forces are considered to be stable in time, therefore, according to Newton's second law of motion, we have a uniform acceleration (denoted by a_z and a_r) in each orthogonal axis as follows:

$$a_z = \frac{Fz}{(\rho_P - \rho_l)Vg} \quad \text{and} \quad a_r = \frac{Fr}{(\rho_P - \rho_l)Vg}. \quad (12)$$

At equilibrium the particles locate in both horizontal and vertical directions and we describe the corresponding displacement of the particle as $(S_{z_i} S_{r_i})$ which is defined by

$$S_{z_i} = \iint_{t_0}^{t_i} a_z d^2t = \iint_{t_0}^{t_i} \frac{Fz}{(\rho_P - \rho_l)Vg} d^2t \quad \text{and} \quad i \in N, \quad (13)$$

$$S_{r_i} = \iint_{t_0}^{t_i} a_r d^2t = \iint_{t_0}^{t_i} \frac{Fr}{(\rho_P - \rho_l)Vg} d^2t \quad \text{and} \quad i \in N, \quad (14)$$

where t_0 and t_i denote the original time and an arbitrary time, respectively.

3 Results and discussion

3.1 Single-particle experiment

As MnCl_2 solution is paramagnetic, it will be attracted close to the magnetic field centre, which leads to the slight distortion of the liquid surface [13]; this has been observed during the experiments as well.

Figure 3 presents the horizontal deflection of glass particles in a 4M MnCl_2 solution under different magnetic fields from 9.5 T to 16.5 T, which is a typical phenomenon of particle horizontal deflection in a magnetic fluid. The glass particle was dropped into the container at the point above the angle position. The X axis indicates the length of the glass box, which is about 195 mm and the Y axis indicates the height of the glass box, which is about 145 mm. The right side of the figure was one side of the glass box which was close to the magnet bore centre. The left side of the figure is the side of the glass box which is far away from the bore centre.

It can be seen from fig. 3 that the deflection behaviour and trajectory of a particle at different magnetic field strengths was different. The particle was deflected more under a stronger field and took more time to settle to the bottom of the container due to the stronger buoyancy force competing with gravity.

From table 1, it could be seen that as the concentration of MnCl_2 increased, the magnetic susceptibility increased. The effect of decrease MnCl_2 concentration, should be similar with the effect of decrease the magnetic field strength. So, similar with fig. 3 in this paper, the lower contents of MnCl_2 used, the glass particle should be deflected less and took less time to settle down at the bottom of the container due to the relatively weak buoyancy force competing with gravity. The reason why we chose 4M MnCl_2 is to see the deflection path more clearly.

The deflection behaviour of a glass particle with different sizes (diameters) is shown in fig. 4a. It would seem that a glass particle with a diameter of 0.7 mm behaved similarly to that of a 1 mm diameter one which indicates that the size of particle did not have an obvious effect on the horizontal deflection. This supports our assumption

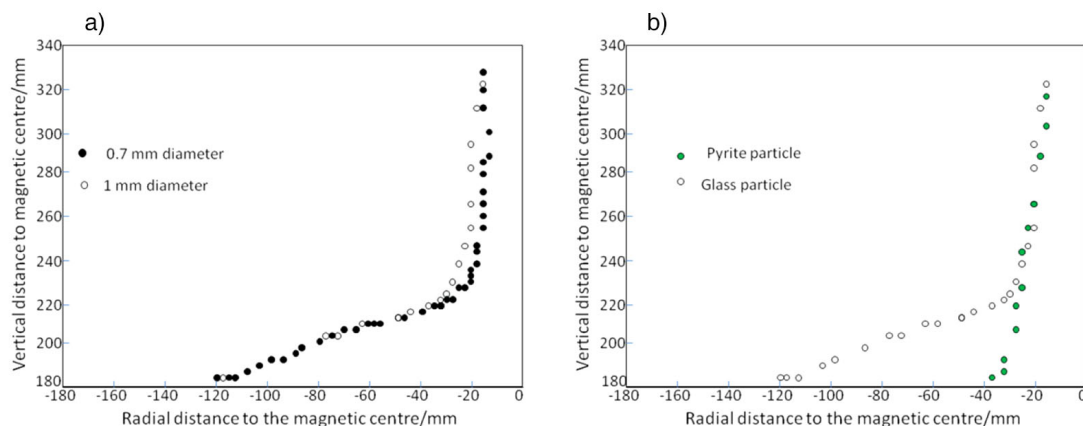


Fig. 4. The deflection of glass and pyrite particle at 16.5 T. a) Glass particle with $d = 1$ mm. b) Glass ($d = 0.7$ mm), pyrite (0.7–1.2 mm).

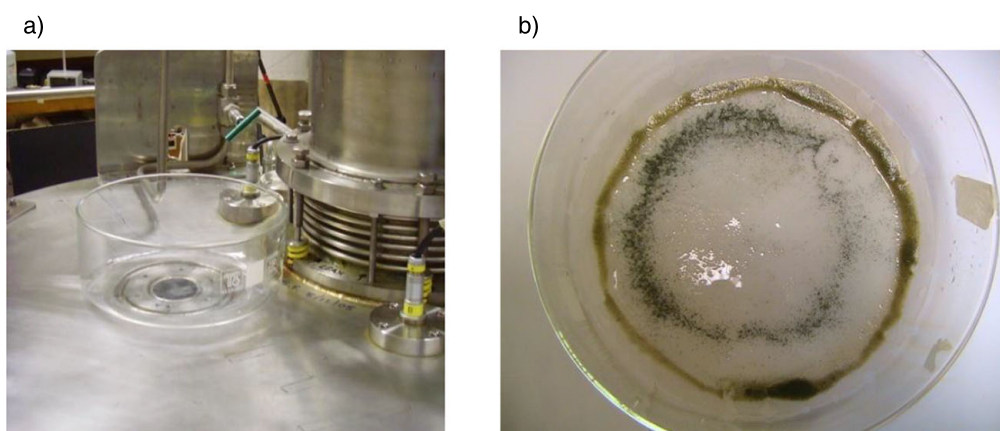


Fig. 5. The deflection of sand and pyrite in cylinder (16.5 T, 4M MnCl_2 , 0.15–0.2 mm). a) Experimental setup. b) Two rings formed in the cylinder.

as the variation of particle size would not change the vertical and horizontal forces balance acting on the particle, thus the influence of particle size on the particle deflection should be negligible.

Several experiments were conducted to explore the deflection of glass and pyrite under similar conditions, which is shown in fig. 4b. It was clear that the pyrite and glass particles were separated as the particles settled down at different positions on the container floor due to the balance between the buoyancy force and gravity.

3.2 Deflection of particles in the cylinder

According to the previous results on the deflection of a single particle in a paramagnetic fluid, it could be presumed that the particles group will tend to show the same deflection behaviour when they were put into the same magnetic system. A cylinder shown in fig. 5a was used to carry out the experiments (the particles were dropped from the top of the magnet bore centre), the result is shown in fig. 5b. Two clear rings were formed in the cylinder due to the deflection movement of particles, the inner ring with a dark colour of pyrite particles and an outer ring of sand particles. The sand particles were deflected further away from

the centre of the cylinder than the pyrite particles, which was due to the force balance between gravity and levitation as well as the unbalanced horizontal force raised by the distribution of the magnetic field. In fig. 5, sand particles which are similar to glass (main compositions of both particles are SiO_2) were used for making the observation of the rings formed easier.

3.3 Simulation results

3.3.1 Forces acting on particles in magnetic field

Based on the equations in sect. 2.5.1, Matlab was chosen to measure the total forces acting on the particles in magnetic field. The total forces acting on glass particle in 4M MnCl_2 solution under the magnetic field of 16.5 T was shown in fig. 6. The arrows point along the direction of the force, while the background colour gives an idea of the value of the modulus. It can be seen that the forces were smaller as the height increased (Z vertical distance from the magnet bore centre) and the radial distance increased (r is the radial distance from the magnet bore centre).

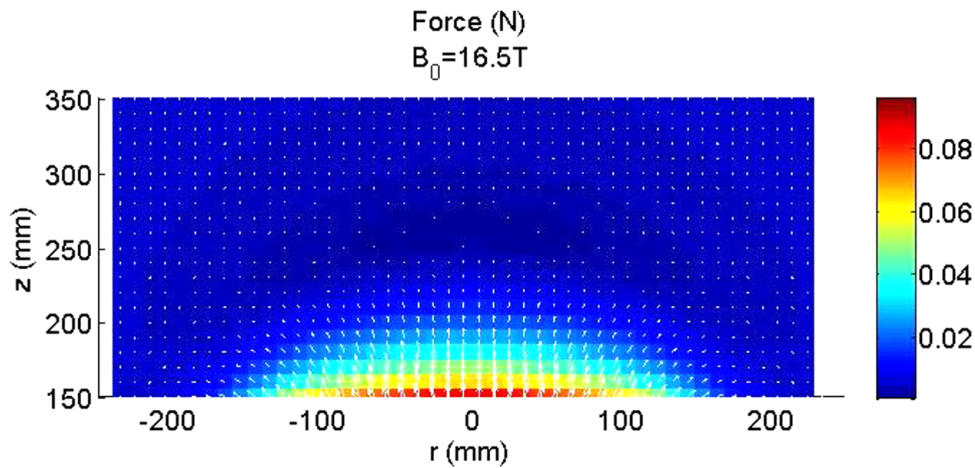


Fig. 6. Forces acting on glass particle ($d = 1$ mm) in magnetic field ($B_c = 16.5$ T).

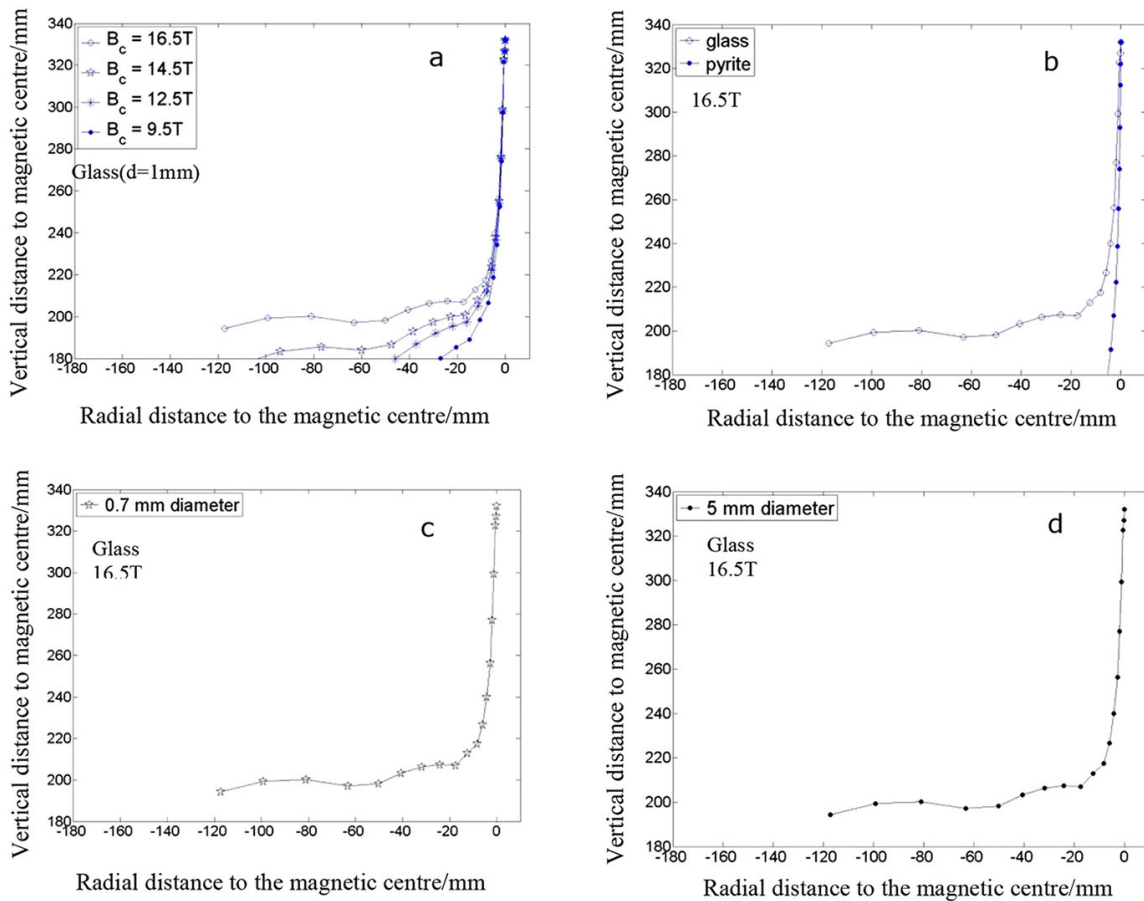


Fig. 7. Simulation results of particle deflection in a magnetic field.

3.3.2 Single-particle movement in magnetic field

It was indicated from the aforementioned experiments that under different magnetic field, the particles were deflected in different paths. The modelling result of this was shown in fig. 7. It is clear again that the glass particle ($d = 1$ mm, fig. 7a) has different deflection path under dif-

ferent magnetic field strength. For stronger magnetic field strength, the glass particle was deflected more and settled at positions away from the bore centre. The different paths of glass particle and pyrite particle were modelled and the results are shown as fig. 7b, which indicate that the pyrite and glass particle were deflected at different paths and settled at certain positions due to the difference of density and magnetic susceptibility.

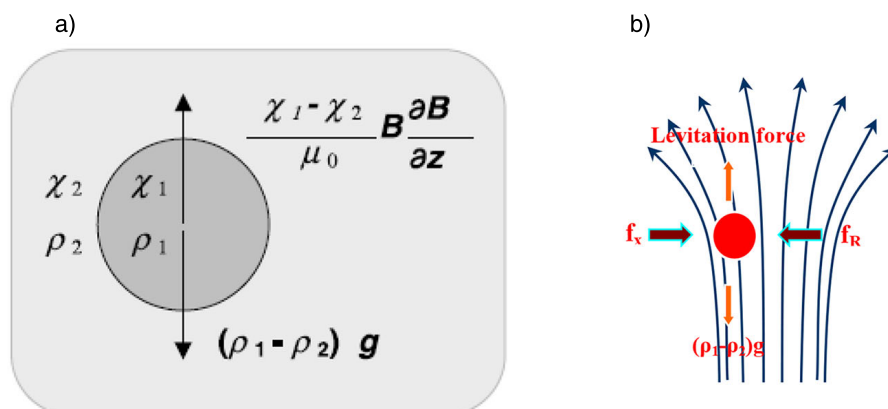


Fig. 8. Forces acting on particles in a magnetic field. a) Forces balance (in the centre). b) Forces balance (deviating from the centre).

The effect of particle size on the horizontal deflection has been modelled as well, the results are shown in fig. 7c and d. It could be indicated that particle size has negligible effect on the horizontal deflection, at least for the size ranged examined in these modelling work (0.7–5 mm). Comparing the modelling work (fig. 7) with the experimental results (fig. 3 and fig. 4), it is clear that the simulation method is reliable and almost got the same trend of particle movement in magnetic field as that in experiments. Thus, presumably, this simulation method could be potentially developed and used to predict the behaviour of particles in a more complicated system.

3.4 Discussion

Separation in magnetic fluids is a sink-and-float technique, which exploits differences in the densities and susceptibilities of materials to be separated. In this technique, a magnetic fluid, placed in a non-homogenous magnetic field, exhibits an apparent density difference from its natural density [8]. This apparent density can be controlled through a wide range of values [13]. The vertical balance of forces (levitation and gravity) on particles could be described by fig. 8a when the particles are sitting in the centre of the magnetic field [5].

However, when it comes to the horizontal deflection, if the particles deviate from the centre of magnetic field (fig. 8b), due to the uneven distribution of magnetic field in the horizontal direction characterized by high density in the middle of magnetic poles and low density at the outside of magnetic poles, two kinds of forces acting on the particle: a magnetic force (f_x , attracting particle toward the centre of magnetic poles) and a magnetic repulsion force (f_R , repelling the particle to the outside magnetic poles). Usually f_R is stronger than f_x , which is the main factor leading to particles horizontal deflection.

Due to the inhomogeneous magnetic field strength, the trajectory of particles will be a curve instead of a straight line.

Experimental results were in good accordance with those of simulation, both of them indicated the horizontal

deflection of particles among magnetic fluid under strong magnetic field, which could be potentially developed to separate particles as per the differences in density and/or susceptibility.

4 Conclusions

The concept of separation of non-magnetic particles suspended in a magnetic fluid is based on the magneto-Archimedes principle whereby, in addition to the conventional force of gravity acting on the fluid, also a magnetically induced force acts on the fluid. This additional magnetic pull creates a magnetically induced buoyancy force on a particle immersed in the fluid. Based on this, a glass box and cylinder were designed to investigate the movement of particles in magnetic fluid. It was found that particles were repulsed to the inner wall of a cylinder to form a ring. Pyrite and glass particles were deflected and settled at certain positions in a specially designed container due to differences in their densities and magnetic susceptibilities. The density and susceptibility of particles, as well as the magnetic field strength, were found to be the major factors influencing the movement of particles. Particle size (diameter) seemed to have little influence on the results, at least for the size range examined in these experiments. Similar results were obtained for experiments and mathematical simulation. It is appreciated that extending this range, particularly to the finer sizes, would increase the influence of other types of forces, *e.g.*, hydrodynamic forces, on the separation behaviour. The horizontal deflection behaviour of the particles provides a new concept for the potential separation of particles. These are very early results and considerable more work is required to understand the basic system, not least the behaviour of fluids that could potentially be used as magneto-Archimedes agents. This work is continuing in collaboration with physicists and is currently exploring a broader range of particle types and sizes as well as potential hydrodynamic forces.

Nomenclature

Variables		Units
a	general acceleration of velocity	(m s ⁻²)
B	magnetic induction field strength	(T)
B_r	horizontal direction magnetic field strength	(T)
B_z	vertical direction magnetic field strength	(T)
B'	vertical direction magnetic field gradient	(T m ⁻¹)
C_{salt}	mass percentage of salt in the total mass	(-)
F	magnetic force per unit mass	(N kg ⁻¹)
F_r	horizontal direction force	(N)
F_z	vertical direction force	(N)
f	general force	(N)
g	acceleration of gravity	(m s ⁻²)
k	volume magnetic susceptibility	(-)
k_p	mass susceptibility of the levitating substances	(-)
k_l	mass susceptibility of the medium gas (or liquid)	(-)
m	mass of the particle	(kg)
S	displacement	(m)
t	time	(s)
U_{mag}	magnetic energy	(m ⁴ T ² H ⁻¹)
V	particle volume	(m ³)
v_t	velocity after time t	(m s ⁻¹)
v_0	velocity at time is zero	(m s ⁻¹)
X	specific magnetic susceptibility	(kg ⁻¹)
x	mass magnetic susceptibility	(m ³ kg ⁻¹)
μ_0	permeability of free space	(H m ⁻¹)
ρ	mass density	(kg m ⁻³)
ρ_p	density of the levitating substances	(kg m ⁻³)
ρ_l	density of medium gas (or liquid)	(kg m ⁻³)
$\frac{dB}{dz}$	vertical direction magnetic field gradient	(T m ⁻¹)
$\frac{dB}{dr}$	horizontal direction magnetic field gradient	(T m ⁻¹)

This work was funded as part of the UK Engineering and Physical Sciences Research Council Basic Technology Programme: Magnetic Levitation Technology for Mineral Separation, Nanomaterials, and Biosystems for Space Exploration (GR/S83005/01).

References

1. J. Svoboda, *Magnetic Techniques for the Treatment of Materials* (Kluwer Academic Publishers, 2004).
2. K. Yokoyama, T. Oka, H. Okada, Y. Fujine, A. Chiba, K. Noto, *IEEE Trans. Appl. Supercond.* **13**, 1592 (2003).
3. R.D. Doctor, C.D. Livengood, <http://www.p2pays.org/ref/14/13875.pdf>, pp. 228–235.
4. H. Okada, H. Okuyama, M. Uda, N. Hirota, *IEEE Trans. Appl. Supercond.* **16**, 1084 (2006).
5. I. Ihara, K. Kanamura, E. Shimada, T. Watanabe, *IEEE Trans. Appl. Supercond.* **14**, 1558 (2004).
6. D. Ito, K. Miura, T. Ichimura, I. Ihara, T. Watanabe, *IEEE Trans. Appl. Supercond.* **14**, 1551 (2004).
7. H. Okada, Y. Kudo, H. Nakazawa, A. Chiba, K. Mitsunashi, T. Ohara, W. Hitoshi, *IEEE Trans. Appl. Supercond.* **14**, 1576 (2004).
8. T. Hartikainen, J. Nikkanenand, R. Mikkonen, *IEEE Trans. Appl. Supercond.* **15**, 2336 (2005).
9. M. Mothokawa, M. Hamai, T. Sato, I. Mogi, S. Awaji, K. Watanabe, N. Kitamura, M. Makihara, *Physica B* **294–295**, 729 (2001).
10. W. Braunbeck, *Z. Phys.* **112**, 735 (1939).
11. E. Baeugnon, R. Tournier, *Nature* **349**, 470 (1991).
12. A.K. Geim, M.D. Simon, M.I. Boamfa, L.O. Heflinger, *Nature* **400**, 323 (1999).
13. M.V. Berry, A.K. Geim, *Eur. J. Phys.* **18**, 307 (1997).
14. Y. Ikezoe, T. Kaihatsu, S. Sakae, H. Uetake, N. Hirota, K. Kitazawa, *Energy Convers. Manage.* **43**, 417 (2002).
15. P.A. Dunne, J. Hilton, J.M.D. Coey, *J. Magn. & Magn. Mater.* **316**, 273 (2007).
16. N. Hirota, M. Kurashige, M. Iwasaka, M. Ikehata, H. Uetake, T. Takayama, H. Nakamura, Y. Ikezoe, S. Ueno, K. Kitazawa, *Physica B* **346**, 267 (2004).
17. R.E. Rosenweig, *Nature* **210**, 613 (1966).
18. R.E. Rosenweig, *AIAA J.* **4**, 1751 (1966).
19. R.E. Rosenweig, *Ferrohydrodynamics* (Dover publications, New York, 1997) ISBN 0-486-67834-2.
20. L. Mir, C. Simard, S.D. Grana, in *Proceedings of the 3rd Urban Technol. Conf. Tech. Display, Boston (USA)*, AIAA Paper no. 73-959 (1973).
21. T. Fujita, in *Magnetic Fluids and Applications Handbook*, edited by B. Berkovski, V. Bashtovoy (Begell House, Inc., New York, 1996).
22. J. Svoboda, *Phys. Separ. Sci. Eng.* **13**, 127 (2004).
23. A.T. Catherall, L. Eaves, P.J. King, S. Booth, *Nature* **422**, 579 (2003).
24. A.T. Catherall, P. Lopez-Alcaraz, K.A. Benedict, P.J. King, L. Eaves, *New J. Phys.* **7**, 118 (2005).
25. P. Lopez-Alcaraz, A.T. Catherall, R.J.A. Hill, M.C. Leaper, M. Swift, P.J. King, *Eur. Phys. J. E* **24**, 145 (2007).
26. U. Andres, *Miner. Sci. Engin.* **7**, 99 (1975).
27. M. Suwa, H. Watarai, *Anal. Chem.* **74**, 5027 (2002).
28. *Landolt-Börnstein Numerical Data and Functional Relationships in Science and Technology, New Series, II/16, Diamagnetic Susceptibility* (Springer-Verlag, Heidelberg, 1986).
29. G.P. Arrighini, M. Maestro, R. Moccia, *J. Chem. Phys.* **49**, 882 (1968).
30. Y.J. Choi, K.L. McCarthy, M.J. McCarthy, *Comput. Electron Agr.* **47**, 59 (2005).
31. L. Pangione, J.B. Lister, *Fusion Eng. Des.* **83**, 545 (2008).
32. C.L. Lim, N.B. Jones, S.K. Spurgeon, J.J.A. Scott, *Simul. Modell. Pract. Theory* **11**, 91 (2003).
33. Q.X. Feng, Q. Feng, K. Takeshi, *Nucl. Sci. Technol.* **19**, 282 (2008).
34. M.D. Simon, A.K. Geim, *J. Appl. Phys.* **87**, 6200 (2000).